湖南大学学报（自然科学版）
Journal of Hunan University (Natural Sciences)

第 51 卷 第 6 期
2024 年 6 月

Available online at http://jonuns.com/index.php/journal/index

Vol. 51 No. 6
June 2024

Open Access Article

https://doi.org/10.55463/issn.1674-2974.51.6.35

Electromagnetic Wave Absorption Capability and Magnetic Properties of Magnetic Jabon Wood

Istie Rahayu[1]*, Rohmat Ismail[2], Mamay Maslahat[3], Wayan Darmawan[1], Irma Wahyuningtyas[4], Esti Prihatini[1], Gilang Dwi Laksono[1]

[1] Department of Forest Products, Faculty of Forestry and Environment, IPB University, Bogor, Indonesia

[2] Department of Chemistry, Faculty of Mathematics and Natural Sciences, IPB University, Bogor, Indonesia

[3] Department of Chemistry, Faculty of Mathematics and Natural Sciences, Nusa Bangsa University, Bogor, Indonesia

[4] Department of Forest Product Processing Technology, Faculty of Environment and Forestry, Samarinda State Agricultural Polytechnic, Samarinda, Indonesia

* Corresponding author: istiesr@apps.ipb.ac.id

Received: April 11, 2024 / Revised: May 14, 2024 / Accepted: May 21, 2024 / Published: June 30, 2024

Abstract: Magnetic wood was prepared from jabon wood (*Anthocephalus cadamba* Miq.) impregnated with magnetite (Fe_3O_4) nanoparticles produced by the co-precipitation method using NaOH (MG-SB) and NH_4OH (MG-WB) as base precursors. This study aims to characterize the magnetic and physical properties of magnetic jabon wood and its electromagnetic wave absorption behavior. Three levels of magnetite concentration, specifically 1%, 2.5%, and 5%, were submerged in wood for thirty minutes under a vacuum pressure of -0.5 bar, followed by a pressure of 2 bar for two hours. The enhancement of jabon wood's physical properties, including its weight percent gain, bulking effect, anti-swelling efficiency, water uptake, and wood density, was confirmed to have a positive impact. The success of magnetite impregnation into wood was also demonstrated by the presence of magnetite inside the wood cavities by the SEM-EDX analysis and a new peak in FTIR spectra, which indicated the Fe-O functional group. The measurement of XRD spectra indicated an increase in the crystalline area of cellulose. The most important point is that this treatment can also improve the magnetic properties of wood, as seen from the analysis results obtained using Tesla meter, VSM, and VNA instruments. The MG-SB 5% magnetic jabon wood is capable of absorbing 94.71% of electromagnetic waves, while the MG-WB 5% is capable of absorbing 95.55% of electromagnetic waves. Fe_3O_4 nanoparticles not only improve the physical properties of jabon wood, but also expand its intended use, enabling it to become a wood-based advanced material that can absorb electromagnetic waves effectively.

Keywords: *Anthocephalus cadamba*, coprecipitation, magnetite, impregnation, physical properties.

磁性贾本木材的电磁波吸收能力和磁特性

摘要：磁性木材由浸渍了磁铁矿(氧化铁)纳米粒子的日本海棠木(斑头花.)制成，该纳米粒子采用共沉淀法制备，以氢氧化钠(MG-SB)和氨水(MG-WB)为基体前体。本研究旨在表征磁性日本海棠木的磁性和物理特性及其电磁波吸收行为。将三种浓度的磁铁矿（具体为 1%、2.5%和 5%）浸入木材中，在-0.5 巴的真空压力下浸泡 30 分钟，然后在 2 巴的压力下浸泡 2 小时。日本海棠木的物理特性（包括其重量百分比增加、膨胀效果、抗膨胀效率、吸水率和

木材密度）的增强已被证实具有积极影响。磁铁矿浸渍木材的成功还体现在扫描电子显微镜分析中木材腔内存在磁铁矿，红外光谱光谱中出现了一个新峰，表明存在铁氧体官能团。XRD 光谱测量表明纤维素的结晶面积增加。最重要的一点是，这种处理还可以改善木材的磁性，这从使用特斯拉计、向量空间模型和越通社仪器获得的分析结果可以看出。MG-SB 5%磁性巴西木能够吸收 94.71%的电磁波，而 MG-WB 5%能够吸收 95.55%的电磁波。氧化铁纳米粒子不仅改善了巴西木的物理性质，还扩大了其预期用途，使其成为一种能有效吸收电磁波的木质先进材料。

关键词：斑彩花，共沉淀，磁铁矿，浸渍，物理特性。

1. Introduction

Metal nanoparticles have been developed for wood modification in recent decades. It has many advantages, such as high surface-to-volume ratio, uniform particle size distribution, and good stability [1]. Their small size allows them to penetrate the wood pores deeply, thereby increasing the wood's physical-mechanical properties and protecting the wood from UV exposure and biological attacks such as termites, fungi, and molds [2], [3]. Wahyuningtyas et al. [4] modified wood with iron nanoparticles to create a novel material known as magnetic wood, which exhibits paramagnetic properties.

Magnetic wood has been modified to have properties and behaviors similar to those of permanent magnetic materials. Numerous investigations [5], [6] have focused on the production of magnetic wood from fat-growing wood by employing iron nanoparticles, which display exceptional physical-mechanical and magnetic characteristics. This wood is suitable for this treatment due to its poor physical-mechanical properties; thus, the wood is more durable and has a new function. Therefore, this study employs magnetite nanoparticles (Fe_3O_4) as an impregnation material in magnetic wood fabrication. Magnetite is a mineral commonly found with an inverse spinel structure, consisting of oxygen formed in tight cubic packages and iron arranged in tetrahedral and octahedral positions. This structure gives rise to the ferromagnetic and semiconducting properties of magnetite [7].

Magnetite nanoparticles can be manufactured via co-precipitation. In this study, this method involved ammonium hydroxide (NH_4OH) and sodium hydroxide (NaOH) as base precursors. Both base precursors were supplied during manufacture to obtain smaller and similar-sized magnetite nanoparticles [8]. Depositing magnetite nanoparticles in the wood interior is expected to not only improve the basic properties of wood but also expand its intended use. Therefore, this study compared the magnetic and physical properties of magnetic wood made from two different types of magnetite nanoparticles.

2. Materials and Methods

2.1. Materials

The main material used in this study was a 5-year-old with a 25-28 cm diameter of jabon wood (*Anthocephalus cadamba* Miq.) selected randomly from a community plantation forest in Bogor, West Java. The chemicals used in the study included iron (III) chloride tetrahydrate (Merck), iron (II) chloride tetrahydrate (Merck), ethylenediaminetetraacetic acid (EDTA) (Merck), natrium hydroxide (NaOH) (Merck), ammonium hydroxide (NH_4OH) (Merck), hydrochloric acid (HCl) (Merck), universal pH indicator paper (Merck), and demineralized water.

2.2. Methods

2.2.1. Wood Sample Preparation

Jabon wood was cut into 2 cm × 2 cm × 2 cm [9] without recognizing sapwood and heartwood. A total of 70 wood samples were used for 10 replications at each concentration. After treatment, the samples were tested for characteristics and physical properties.

2.2.2. Synthesis of Magnetite (Fe_3O_4) Nanoparticles

The coprecipitation technique was employed to produce magnetite nanoparticles. By combining an iron solution with oxidation numbers 2 and 3 in the form of hydrated chloride salts in an alkaline medium, with a mole ratio of Fe^{2+}/Fe^{3+} = ½, synthesis was carried out. Initially, 10 mL of 1-M EDTA and 10 mL of 2-M HCl were added to prevent the oxidation of Fe^{2+} and precipitation of Fe^{3+} in the hydroxide form. 125 mL of the precursor solution with a molar concentration of 0.30-M Fe^{3+} and 0.15-M Fe^{2+} was mixed and stirred for three minutes. Furthermore, the 1.5-M NH_4OH solution as a weak base precursor precipitate was added gradually to the iron mixture solution until a black precipitate was formed and reached pH 12, while constantly stirring. The resulting black sediment was isolated with a permanent magnet and washed with

demineralized water until pH 9 was reached. The obtained product was separated using a permanent magnet and dried at 40°C for 24 h [10]. The same procedure was used to produce strong base magnetite precipitation, namely using a 1.5-M NaOH solution [11]. This process can be described by Eq. 1 [11]:

$$Fe^{3+} + 3OH^- \rightarrow Fe(OH)_3$$
$$Fe(OH)_3 \rightarrow FeOOH + H_2O \quad (1)$$
$$Fe^{2+} + 2OH^- \rightarrow Fe(OH)_2$$
$$2FeOOH + Fe(OH)_2 \rightarrow Fe_3O_4 + 2H_2O$$

2.2.3. Wood Impregnation

Before initiating the impregnation, the solution was homogenized using an ultrasonic homogenizer (300W CGOLDENWALL 5-200MLLab, Zhejiang, China) with amplitude of 40% for 60 min. Impregnation was carried out at three concentrations of the magnetite nanoparticles: 1, 2.5, and 5% (w/v%). Jabon wood samples were immersed in these solutions in an impregnation tube with a vacuum of -0.5 bar for 0.5 h and a pressure of 2 bar for 2 h. Following this process, the wood samples were rinsed with demineralized water to remove the remaining solution and then wrapped in aluminum foil. This process was continued by heating the wood samples at 65°C for 12 h for polymerization and drying at 105°C for 48 h until reaching a constant weight.

2.2.4. Physical Property Test

After the impregnation process, the wood's physical properties including weight percent gain (WPG), anti-swelling efficiency (ASE), water uptake (WU), bulking effect (BE), and density (ρ) were evaluated using Eq. 2–6.

$$WPG\ (\%) = [(W_1 - W_0)/W_0] \times 100 \quad (2)$$
$$ASE\ (\%) = [(S_u - S_t)/S_u] \times 100 \quad (3)$$
$$WU\ (\%) = [(W_2 - W_1)/W_1] \times 100 \quad (4)$$
$$BE\ (\%) = [(V_1 - V_0)/V_0] \times 100 \quad (5)$$
$$\rho\ (kg/m^3) = W_1/V_1 \quad (6)$$

Notes:

W_0 - initial mass of wood before impregnation
W_1 - final mass of wood after impregnation
W_2 - wood mass after 24 h of water soaking
S_u - volume shrinkage of untreated wood
S_t - volume shrinkage of impregnated wood
V_0 - initial wood volume before impregnation
V_1 - final wood volume after impregnation

2.2.5. Magnetic Wood Particle Size Analyzer (PSA)

A substance containing 10 mg of synthetic magnetite nanoparticles was dissolved in 100 mL of demineralized water and stirred using a sonicator for 15 min. A PSA (Beckman Coulter LS 13 320 XR) was used to measure the diameter of the magnetite nanoparticle at a concentration of 100 ppm.

2.2.6. Scanning Electron Microscopy (SEM)-Energy Dispersive X-Ray Spectroscopy (EDS)

The SEM Zeiss EVO10 series was utilized to examine the morphology of the jabon wood. The wood samples were tangentially sliced into 0.5 cm × 0.5 cm × 0.5 cm. The process entailed laying wood samples on a conductive adhesive, applying gold as the electrically conductive metal, and observing at voltage of 20 kV. The chemical contents of the treated wood were determined by EDS analysis using ZEISS SmartEDX.

2.2.7. Fourier Transform Infrared (FTIR) Spectrometry

The wood samples were processed to a particle size of 200 mesh and then combined with potassium bromide (KBr) pellets at a ratio of 1:100. A resolution of 4 cm^{-1} was employed for 32 scans to analyze the pellets using FTIR (Perkin Elmer Spectrum One) within the range of 4000-400 cm^{-1}.

2.2.8. X-Ray Diffraction (XRD) Spectrometry

To evaluate the crystallinity of the wood samples and the size of the magnetite in the treated wood, the samples were cut using a 2-mm-thick cutter in a tangential plane. The equipment utilized included a Cu Kα radiation source, a graphite monochromator, with voltage of 40 kV and current of 30 mA. The scanning range was set at 2°/minute in the range of 2θ from 5 to 90°.

2.2.9. Teslameter

Fig. 1 illustrates the wood sample for magnetic strength measurement using this instrument. The wood was drilled on each side with a diameter of 10 mm. This sample was designed to explain the direction of magnetic properties based on surface area A, section area B, and the edges of surface area C.

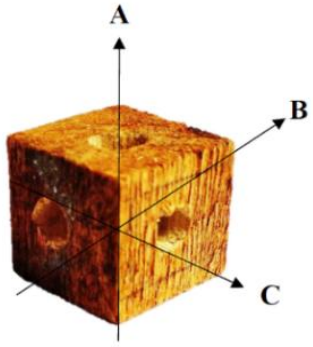

Fig. 1 Schematic of wood sample preparation for magnetic property measurements (The authors)

2.2.10. Vibrating Sample Magnetometer (VSM)

The other parameters of the magnetic wood evaluated in this study were saturation magnetization (Ms), retentivity (Mr), and coercivity (Hc). These magnetic properties were determined by characterizing the wood samples using a VSM Dexing Type 250. Hysteresis loops were generated in an external magnetic field ranging from 100 Oe to 21 kOe at 298–773 K. The longitudinal cross-sectional dimensions of the samples were 3.5 mm × 3.5 mm × 1 mm.

2.2.11. Vector Network Analyzer (VNA)

The microwave absorption of the wood was conducted using a vector network analyzer (VNA) Advatest-R3370 (Fig. 2). The frequency range was 8–20 GHz. To generate reflection loss, measurements were conducted using scattering electromagnetic wave (EMW) parameters from S_{11} models.

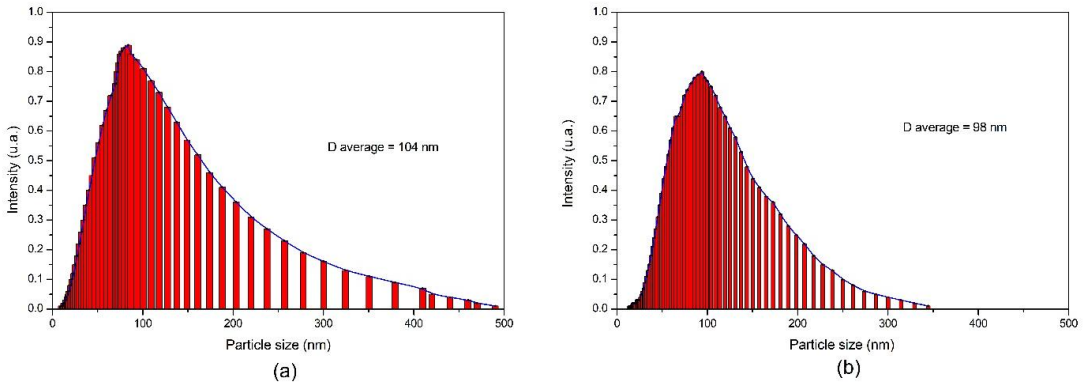

Fig. 2 Size distribution of magnetite nanoparticles synthesized by the coprecipitation method using (a) a strong base precursor and (b) a weak base precursor (The authors)

2.3. Data Analysis

IBM SPSS Statistics 25 (Statistical Package for the Service Solutions) used a completely randomized design to analyze the results. ANOVA, with Duncan's level of accuracy set at 0.05, was implemented in this study. The analysis was supported by the use of the Origin 8.5 software to process characterization data.

3. Results and Discussion

3.1. Characteristics of Magnetite Nanoparticles

In the synthesis of magnetite nanoparticles, strong base NaOH (MG-SB) and weak base NH_4OH (MG-WB) were used as precursors, and EDTA was used as a coating agent. The choice of EDTA was based on its capacity to control the growth of the magnetite core, resulting in smaller and more uniformly shaped magnetite particles [8]. EDTA is believed to improve the stability of magnetite nanoparticles, reduce its activation energy during particle-forming reactions, which promote nucleation, and produce nanosized materials with high absorption capacity and surface area [12]. To verify these statements, PSA was performed to determine the particle size of individual magnetite nanoparticles produced using strong and weak base precursors. This analysis provided various particle size distribution data (Fig. 2).

The distribution of particle size for magnetite nanoparticles synthesized using a strong base NaOH precursor was found to range from 10 to 490 nm, with a corresponding average size of 103 nm and highest intensity observed at 84 nm. In contrast, magnetite nanoparticles synthesized with a weak base precursor exhibited a particle range of 13 to 344 nm, with a highest intensity of 94 nm and average size of 98 nm. As a result, synthetic magnetite nanoparticles can be considered as nanoparticles, particularly when the particle size is within the range of 1 to 100 nm and the crystal size approaches [13]. In agreement with Peternele et al. [10], magnetite nanoparticles synthesized with a weak base precursor exhibit a more uniform particle distribution range and smaller average particle size than those synthesized with a strong base precursor.

3.2. Physical Properties of Magnetic Wood

The findings are presented in Table 1, with untreated wood serving as the control comparison. The highest WPG in the MG-SB wood samples was attained with the 2.5% MG-SB. Although there was a slight increase in the WPG of treated wood, it is significantly different from that of untreated wood. This also means that the concentration of the solution is not necessarily proportional to the magnetite content in the impregnated jabon wood. This is caused by the residual nature of the strong base NaOH. In this case, residual hydroxyl ions can improve the solubility of magnetite in water by forming hydrogen bonds, but residues of sodium metal ions at higher concentration levels cause their solubility to reduce [11]. Conversely, the highest WPG in the MG-WB wood samples was attained by the MG-WB 5% solution, implying that the concentration of the solution was directly proportional to the amount of magnetite nanoparticles impregnated into the jabon wood.

Table 1 Physical properties of impregnated jabon wood (The authors)

Treatment	Density (g/cm^3)	WPG (%)	BE (%)	WU (%)	ASE (%)
Untreated	0.32±0.01^{a}	0.00±0.00^{a}	0.00±0.00^{a}	138.99±8.52^{a}	0.00±0.00^{a}
MG-SB 1%	0.33±0.01^{b}	7.49±0.49^{c}	3.22±0.85^{c}	105.49±2.54^{cd}	55.77±8.28^{c}
MG-SB 2.5%	0.33±0.01^{b}	8.85±0.59^{d}	3.64±0.98^{c}	96.28±3.03^{d}	61.03±3.56^{c}
MG-SB 5%	0.33±0.01^{b}	7.62±0.44^{c}	3.40±0.25^{c}	105.40±9.35^{cd}	58.17±6.21^{c}
MG-WB 1%	0.33±0.01^{b}	5.93±0.27^{b}	1.75±0.48^{b}	120.19±7.40^{b}	45.28±9.38^{b}
MG-WB 2.5%	0.33±0.01^{b}	7.41±0.46^{c}	2.28±0.73^{b}	114.22±8.97^{bc}	46.35±8.35^{b}
MG-WB 5%	0.33±0.01^{b}	7.78±0.63^{c}	3.35±0.97^{c}	110.05±0.63^{c}	54.52±7.13^{c}

$^{a-d}$ Significance based on Duncan's test
MG-SB - magnetite synthesized using a NaOH precursor
MG-WB - magnetite synthesized using a NH_4OH precursor

Wood impregnation using nanomaterials not only increases the WPG, but it also enhances the bulking of the lumen cell, which has an effect on the swelling of

the wood cell wall. This is demonstrated by the number of BEs observed in jabon wood after impregnation. As a result, the ASE is increased because magnetite nanoparticles are embedded and cross-linked with the cell wall polymers, thereby preventing wood shrinkage activity [3]. Therefore, it prevents its long-term water sorption behavior considering that the WU of both types of magnetic wood shows a downward trend in contrast with the WPG and BE and makes the wood more dimensionally stable and protected from deterioration.

Nevertheless, the incorporation of magnetite nanoparticles in different concentrations resulted in a consistent increase in wood density across all treatments. This contradicts the findings of Fadia et al. [6], which demonstrated an increase in wood density upon the addition of magnetite concentrations. It is speculated that excessive accumulation of magnetite nanoparticles in certain areas of the wood results in aspirated bordered pits, which obstruct the wood cavities and hinder the compaction of magnetic wood. This is not surprising given that the pore diameter of jabon wood ranges from 130 to 220 μm [14]. Nonetheless, based on the analysis and statistical tests, the most effective treatments for improving the physical properties of jabon wood are the MG-SB 2.5% and MG-WB 5% wood.

3.3. Microstructure of Magnetic Wood

The wood characteristic tests were carried out on each wood sample at the highest concentration, 5%. The notion that magnetite nanoparticles occupied the wood pores was corroborated by the visual transformation of jabon wood to a darker hue, as evidenced in Fig. 3. The untreated wood did not show any discoloration because no chemicals other than water were applied (Fig. 3a). Different effects occur for the MG-SB and MG-WB wood. After adding magnetite nanoparticles to the solution, hydrogen bonding and van der Waals's force dominate in binding the magnetite nanoparticles and lignin components inside the wood cell wall [15]. It was allegedly due to the increase in heating temperature, which impacted polymerization and led to the gradual degradation of hemicellulose [16]. MG-SB wood has a darker color than MG-WB wood, which is associated with a higher WPG. The magnetic wood was subjected to in-depth investigations, which were carried out using an SEM at different magnifications, as depicted in Fig. 3. The presence of magnetite nanoparticles in the magnetic wood is evidenced by the yellow color.

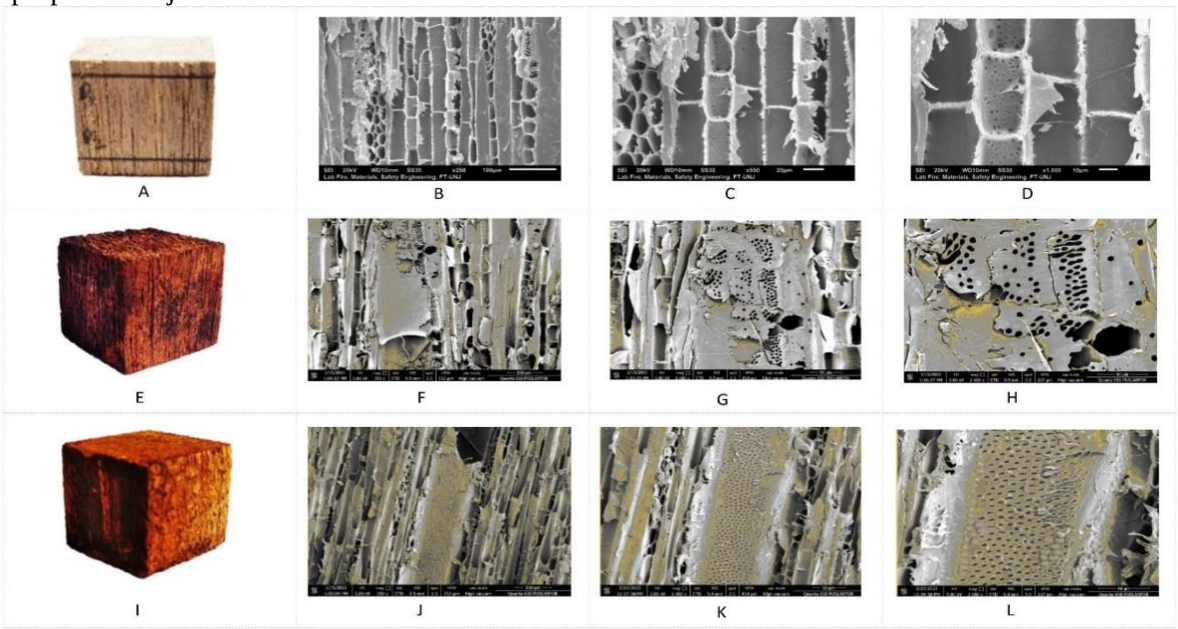

Fig. 3 Morphology of jabon wood: (a) untreated wood, (b) 100× untreated wood, (c) 250× untreated wood, (d) 550× untreated wood, (e) MG-SB, (f) 100× MG-SB, (g) 250× MG-SB, (h) 550× MG-SB, (i) MG-WB, (j) 100× MG-WB, (k) 250× MG-WB, and (l) 550× MG-WB (The authors)

Fig. 3b-d show the absence of magnetite nanoparticles deposited and filled in the wood lumens of the untreated wood. On the other hand, some magnetite nanoparticles were found in the wood vessels, fibers, dots, and cell walls of the MG-SB (Fig. 13f-h) and MG-WB (Fig. 3j-l) wood samples. This justifies the statement that magnetite nanoparticles act as bulking agents and increase wood density, so they have a positive effect on wood dimensional stability. Given the nanometer scale of the particles, there is a strong likelihood that they will effectively penetrate and fill the wood's cavities [17]. To support the SEM analysis, the chemical components responsible for the formation of magnetic wood are presented in the EDS results (Table 2).

Table 2 Chemical components of magnetic wood (The authors)

Wood Sample	Fe (wt. %)	O (wt. %)	C (wt. %)
MG-SB 5%	1.7	46.4	51.9
MG-WB 5%	2.6	47.2	50.2

MG-SB - magnetite synthesized using a NaOH precursor

MG-WB - magnetite synthesized using a NH4OH precursor

Based on Table 2, the MG-WB 5% wood had a higher Fe content than the MG-SB 5% wood. This result contradicts Rahayu et al. [18], who concluded that the utilization of a NaOH precursor resulted in the production of a greater quantity of magnetite nanoparticles that were embedded within the wood cell wall. This process also generated residual sodium metal ions, which led to a reduction in the solubility of the magnetite nanoparticles and resulted in an inhomogeneous composition. This prevented the magnetite nanoparticles from penetrating the wood cavities [11]. Moreover, the WPG of MG-WB 5% wood was higher than that of MG-SB 5% wood because more magnetite nanoparticles were deposited in the interior of the MG-WB 5% wood. Magnetite nanoparticles that infiltrate wood prevent the wood-water interaction and improve the wood's physical properties [5].

3.4. Chemical Analysis of Magnetic Wood

The outputs produced from this instrument are spectra showing the functional groups that can be investigated in the materials (Fig. 4). Coates [19] detected a functional group in untreated wood, such as the absorption bands at 626 cm^{-1} which is known as the tendency of the C-H functional groups. This functional group was found in the lignin aromatic framework. Another peak also recognized as the C-H stretching at a wavenumber of 2909 cm^{-1} represented cellulose and hemicellulose of jabon wood. The finding of the C-O group at 1050 cm^{-1} is associated with the hemicellulose chain of jabon wood [20]. The presence of a C=C functional group at 1653 cm^{-1} also appeared in the untreated wood. At the same time, the O-H peak was identified at 3426 cm^{-1} also indicating the presence of cellulose in jabon wood.

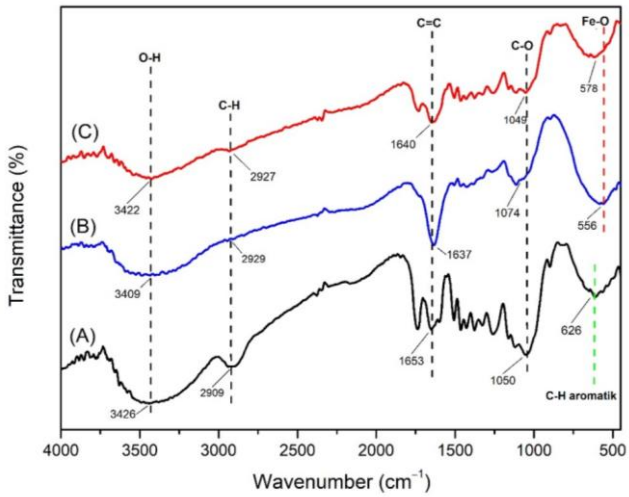

Fig. 4 FTIR spectra of (a) untreated wood, (b) MG-SB 5%, and (c) MG-WB 5% (The authors)

All the functional groups that were discovered in the untreated wood were also present in the MG-SB 5% and MG-WB 5% magnetic wood. The inclusion of magnetite nanoparticle concentration in MG-SB 5% and MG-WB 5% demonstrated the absence of C-H functional groups in the aromatic chains. It is widely held that magnetic nanoparticles encompass the surfaces of cellulose, hemicellulose, and lignin, which constitute the primary polymers comprising the structure of jabon wood [21]. This has an impact on the infrared radiation that is blocked by magnetite nanoparticles, causing the C-H intensity to decrease. The results of this study also revealed that magnetite nanoparticles are only used to bulk up wood pores [1]. To prove this statement, a new peak emerged in the MG-SB 5% and MG-WB 5% magnetic wood, which indicated successful bond formation between the wood polymer and magnetite nanoparticles, consecutively at wavenumbers of 556 and 578 cm^{-1}.

3.5. Magnetic Wood Crystallinity

The XRD analysis results for the jabon wood are shown in Fig. 5. The diffractogram of the untreated wood samples exhibits several peaks indicating the cellulose structure of jabon wood, precisely at 2θ = 15.30°, 21.971°, and 34.1°. Similarly, the 5% wood in the MG-SB sample exhibited the characteristic peaks of cellulose structure at 2θ = 15.49°, 21.96°, and 33.93°. Meanwhile, the 5% wood in the MG-WB sample displayed the peaks at 2θ = 15.11°, 21.71°, and 33.98°. These peaks are identified as crystal planes of I_{020}, I_{012}, and I_{131}, confirmed by the JCPDS standard of the cellulose diffractogram No. 03-0226. The crystal lattices in these peaks, as observed by Osman et al. [22], remained the same even when compared to the control sample. The intensity of I_{131} was weakened in the MG-SB 5% and MG-WB 5% samples, which were thought to be damaged by the magnetic treatment [3]. Despite this, the impregnation treatment did not significantly alter the cellulose crystalline structure, which is the main constituent of jabon wood.

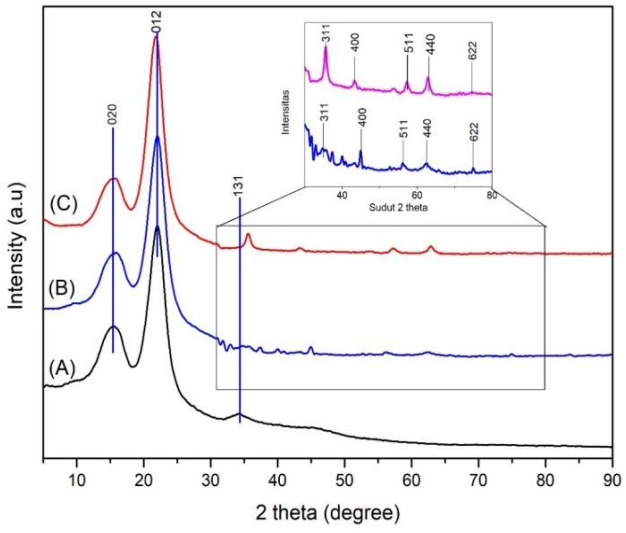

Fig. 5 Diffractograms of (a) untreated, (b) MG-SB 5%, and (c) MG-WB 5% wood (The authors)

Fig. 5 also reveals some new peaks in the MG-SB 5% and MG-WB 5% treated jabon wood. The appeared peaks include 2θ = 35.14°, 44.56°, 56.13°, 62.43°, and 75.05° detected in the MG-SB 5% wood, as well as the diffractogram of the MG-WB 5% wood also shows 2θ = 35,60°, 43.23°, 57.24°, 62.88°, and 74.85°. These peaks belong to the crystal planes of I_{311}, I_{400}, I_{511}, I_{440}, and I_{622}, which justifies the existence of magnetite nanoparticles based on the JCPDS standard comparison of magnetite diffractogram No. 19-0629.

The diffractogram displayed in Fig. 5 was also used to measure the degree of crystallinity and magnetite crystallite size, as reported in Table 3. The modification of the cellulose structure in the amorphous phase during impregnation and the accumulation of inorganic particles, specifically magnetite nanoparticles that form on the surface of the cellulose, result in an increase in crystallinity and crystallite size [23]. It is believed that the magnetite nanoparticles interact with wood polymers and weaken the hydrogen bonds between them. The solution is thought to break the pyranose ring and depolymerize the crystal structure of cellulose [4]. Thus, the amorphous area of wood polymers can be replaced with crystalline magnetite nanoparticles, which exhibit higher crystallinity, as shown in Table 2. An improvement in the crystallinity of wood cellulose typically correlates with a rise in the mechanical strength of the wood [24].

Table 3 Jabon wood crystallinity and magnetite crystal size (The authors)

Treatments	Degree of Crystallinity (%)	Magnetite Crystal Size (nm)
Untreated	60.43	–
MG-SB 5%	70.16	26.13
MG-WB 5%	69.97	29.77

MG-SB - magnetite synthesized using a NaOH precursor
MG-WB - magnetite synthesized using a NH_4OH precursor

The magnetite crystal size was measured using the Scherrer equation (Eq. 7).

$$D = \frac{K\,\lambda}{\beta \cos\theta} \quad (7)$$

This equation describes the relationship between the crystal size (D) and the widening of the diffraction peak (β), which is known as the full width at half maximum (FWHM) of the peak. The X-ray's wavelength (0.15418 nm) is denoted by λ. K is the Scherrer constant (0.89), and θ is the Bragg diffraction angle [23]. The results indicate that the magnetite crystal size measured inside the jabon wood was smaller than the initial magnetite size before the impregnation treatment was conducted. This was due to previously conducted sonication, which can reduce the magnetite particle size [25].

3.6. Teslameter

The magnetic strengths of the impregnated jabon wood are showcased in Table 4, as recorded by the Teslameter instrument. The results show a significant improvement compared with untreated wood. Untreated wood exhibits zero magnetic strength as it is a diamagnetic material. However, when jabon wood is impregnated with magnetite nanoparticles, its magnetic strength increases in direct proportion to the concentration of magnetite. These values are lower than the magnetic strength of magnetite nanoparticles, namely 7.51±0.59 mT for the MG-SB and 8.58±0.63 mT for the MG-WB samples. This phenomenon can occur because diamagnetic cellulose blocks the magnetite in wood pores, thereby reducing its surface magnetic strength [26], [27]. Thus, the optimal treatments for attaining the highest magnetic strength in MG-SB and MG-WB wood were 2.5% and 5% concentrations, respectively.

Table 4 Magnetic strength of jabon wood after impregnation treatment, evaluated using a Teslameter (The authors)

Treatment	Magnetic Strength (mT)
Untreated	0.00 ± 0.00^{a}
MG-SB 1%	0.34 ± 0.01^{b}
MG-SB 2.5%	0.44 ± 0.06^{c}
MG-SB 5%	0.36 ± 0.01^{b}
MG-WB 1%	0.66 ± 0.05^{d}
MG-WB 2.5%	0.81 ± 0.06^{e}
MG-WB 5%	0.91 ± 0.11^{f}

[a-f] Significance based on Duncan's test
MG-SB - magnetite synthesized using a NaOH precursor
MG-WB - magnetite synthesized using a NH_4OH precursor

The magnetic strength obtained from this instrument is closely related to the WPG of the magnetic wood, which represents the number of magnetite nanoparticles penetrating the jabon wood, as shown in Fig. 6, although it has a different range of magnetic strength values. The coefficient of determination is close to 1. This outcome aligns with those by Gao et al. [26], who agreed that the more magnetite impregnated into the wood, the greater the magnetic force produced. Through this test, the magnetic properties of jabon wood were confirmed by the immobilization of magnetite nanoparticles. These findings can serve as a basis for assessing the feasibility of innovative materials in the fabrication of magnetic wood. Calibration of the probe sensitivity tensor was routinely carried out before the analysis began to avoid inaccuracies in the magnetic strength readings.

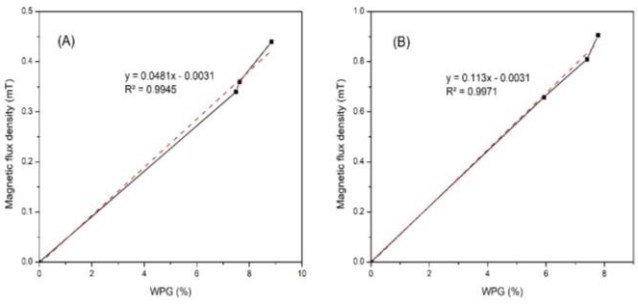

Fig. 6 Correlation curves between the WPG and magnetic fields of jabon wood impregnated with (a) MG-SB and (b) MG-WB (The authors)

3.7. Vibrating Sample Magnetometer (VSM)

Fig. 7 represents the hysteresis loops of the magnetic wood prepared using synthetic magnetic nanoparticles. The presence of strong base (NaOH) and weak base (NH_4OH) precursors in the co-precipitation method is a crucial factor in determining the properties of magnetite nanoparticles. Herein, an elongated and narrow loop was identified as the hysteresis loop of MG-WB 5%. A different shape was observed in the other loop, which tended to be flat, and was identified as the loop of the MG-SB 5% wood sample. The configuration of this loop is reminiscent of the form of the loop observed in untreated wood, which demonstrates diamagnetic behavior characterized by a straight loop shape along the x-axis of the hysteresis curve, as indicated by Moya et al. [28]. By this loop, the value of magnetization saturation (Ms), remanence (Mr), and coercivity (Hc) can also be measured, as listed in Table 5.

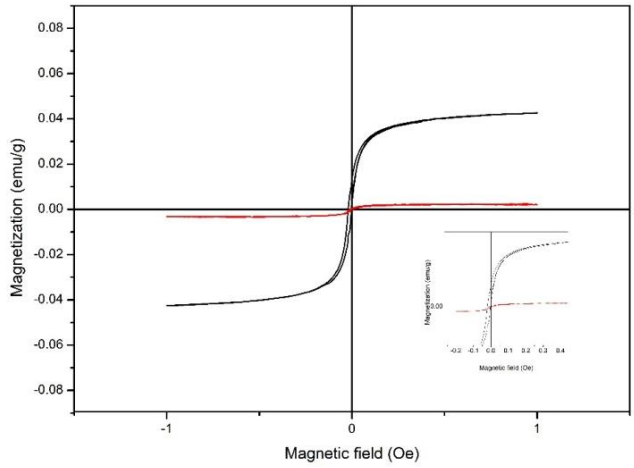

Fig. 7 Hysteresis loops of magnetic wood synthesized using NaOH and NH_4OH (The authors)

Table 5 VSM analysis of magnetic jabon wood (The authors)

Wood Sample	Ms (emu/g)	Mr (emu/g)	Hc (Oe)
MG-SB 5%	0.0021	1.04×10^{-4}	2.18×10^{-5}
MG-WB 5%	0.0425	1.02×10^{-2}	8.6×10^{-3}

MG-SB - magnetite synthesized using a NaOH precursor
MG-WB - magnetite synthesized using a NH_4OH precursor

The MG-WB 5% exhibited higher magnetization than the MG-SB 5%. Although weak base magnetite nanoparticles resulted in larger particle sizes, they were believed to break down into smaller particles upon passing through the narrow wood pores. Moreover, the vacuum pressure impregnation method was employed to promote the penetration of particles into the wood at a deeper level [29]. As a result, they distributed more strongly and uniformly inside the jabon wood after being impregnated into the wood. It is proven by magnetic wood SEM-EDX results; hence, it requires only a small external magnetic field to convert jabon wood into magnetic wood [27]. A similar loop was also obtained by Rahayu et al. [18] when manufacturing magnetic wood using the same precursors. Although the result of this study was lower, both magnetic woods still exhibited superparamagnetic behavior. This condition occurred because the infiltration of magnetite nanoparticles into the wood was believed to be below its critical diameter, which is generally within the range of 10-30 nm. Therefore, magnetite nanoparticles can move in a simple direction at different speeds [30]. It has also been proved that Magnetic wood exhibits a rapid response to applied magnetic fields and possesses a high degree of magnetization that reaches its saturation point with ease. Endowed with these qualities, magnetic wood demonstrates negligible residual magnetism and zero coercivity upon demagnetization [31].

EDTA is very helpful in controlling the magnetite particle size and coating its surface area. The aim is to enhance the stability of magnetite nanoparticles and reduce the possibility of oxidation and agglomeration [12]. The use of EDTA in wood treatment facilitates particle encapsulation and reduces surface energy, thereby ensuring effective dispersion and penetration into the wood [32]. Previous studies [3], [10] have observed the saturation magnetization (Ms) of bulk magnetite nanoparticles, namely 60 emu/g for magnetite synthesized using strong base NaOH and 78 emu/g for magnetite synthesized using weak base NH_4OH. The findings of this study indicate that the magnetic properties of the magnetic wood are lower than those of bulk magnetite due to the presence of magnetite nanoparticles, which have ferromagnetic characteristics but are coated with wood cellulose, which has diamagnetic properties. This results in a negative impact on its magnetic performance [27]. Additionally, the synthesis using NaOH precursor resulted in smaller magnetite nanoparticles, but this does not preclude the possibility of them agglomerating with other particles and forming larger ones [10]. Consequently, the MG-SB 5% was more difficult to magnetize than the MG-WB 5% due to its lower Ms value, which makes it more challenging to magnetize. Nevertheless, the wood sample was able to accommodate a small external magnetic field.

The results revealed a higher remanence and coercivity in the MG-WB 5% wood sample (Table 5). It was hypothesized that a greater number of magnetite nanoparticles had penetrated and cross-linked with the components of the wood cell wall. The particle size and crystallites of the material play a crucial role in determining its saturation magnetization. Its high density leads to a material with numerous crystals, resulting in extensive magnetic regions. Moreover, the magnetite nanoparticles' susceptibility to air exposure could contribute to oxidation and corrosion [3]. Perfect correlation between WPG and Ms is shown in Fig. 8.

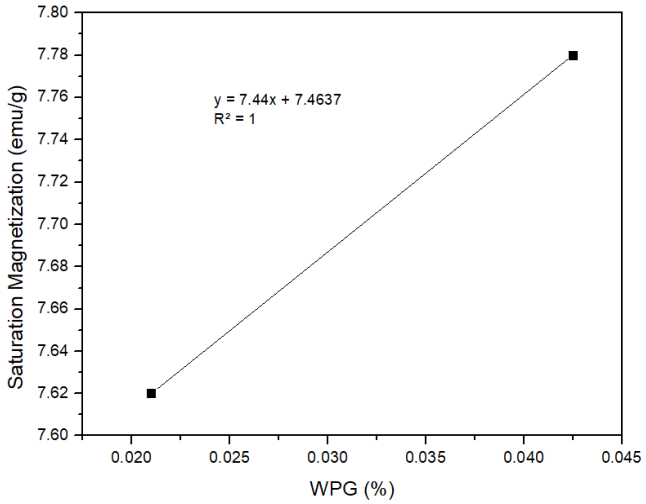

Fig. 8 Correlation between saturation magnetization and WPG of magnetic wood (The authors)

3.8. VNA

The wave-like behavior is produced by a pair of EMWs spreading in the air medium and a perpendicular electric field that charges them [33]. The scattering parameter (S-parameter) used in this test was S_{11}. The frequency range of 8–12 was used to obtain the reflection loss (R_L) and absorption properties of magnetic wood. According to Johan et al. [34], Equations 8-11 were used to calculate the EMW absorption of magnetic wood:

$$Z_{in} = \sqrt{\frac{\mu_r}{\varepsilon_r}}\ tanh\left[j\left(\frac{2\pi fd}{c}\right)\sqrt{\mu_r \varepsilon_r}\right] \quad (8)$$

$$\Gamma| = \frac{Z_{in} - Z_o}{Z_{in} + Z_o} \quad (9)$$

$$\text{Reflection Loss (dB)} = 20 \log |\Gamma| \quad (10)$$

$$\text{EMW absorption (\%)} = (1 - \Gamma^2)\ x\ 100\% \quad (11)$$

where Z_{in} is the material's impedance input, Z_0 is the impedance value under vacuum conditions, ε_r and μ_r respectively represent the relative permittivity and permeability of the medium, f is the microwave frequency, d is the thickness of the absorber, c is the light speed, and $|\Gamma|$ is the wave reflection coefficient.

The R_L results for magnetic wood under various transmission parameters are depicted in Fig. 9. Untreated wood displays the reflection parameter S_{11} value of zero for frequencies ranging from 8 to 12. This is due to the absence of magnetite nanoparticles in the wood, resulting in the absence of EMW absorption by the sample. Another condition experienced by the MG-SB 5% and MG-WB 5%. At a frequency of 8.00 GHz, the MG-SB 5% has an R_L value of -12.77 dB, whereas the R_L value of the MG-WB 5% is -13.52 dB at a frequency of 8.28 GHz. The results indicate that the MG-WB 5% demonstrated a greater capacity for absorbing higher EMW, surpassing the MG-SB 5% with an absorption rate of 95.55%. In contrast, the MG-SB 5% showed an absorption rate of 94.71%. The reduced values of R_L, frequency, and absorption capacity of the MG-SB 5% wood are attributed to the absence of a dielectric material, resulting in a weak capacity for EMW pollution absorption. Various attributes, including shape, properties, and size, influence the increase in R_L and frequency. These factors encompass the wood's microstructure, the interaction between the wood and water molecules, dielectric behavior, material thickness (film viscosity), magnetic permeability index, and complex permittivity [35]. The detailed results are listed in Table 6.

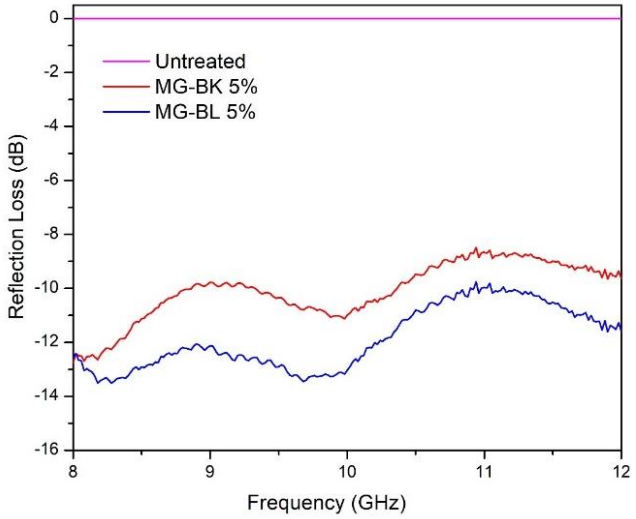

Fig. 9 Relation between reflection loss and frequency of the magnetic wood sample (The authors)

Table 6 VNA results for magnetic jabon wood (The authors)

Treatments	Reflection Loss (dB)	Frequency (GHz)	Absorption (%)
Untreated	0.00	8.00	0.00
MG-SB 5%	-12.77	8.00	94.71
MG-WB 5%	-13.52	8.28	95.55

MG-SB - magnetite synthesized using a NaOH precursor
MG-WB - magnetite synthesized using a NH_4OH precursor

The use of the weak base NH4OH precursor helped to level out the size of the magnetite nanoparticles and facilitated their crystallization, thereby increasing the absorbance capacity of magnetic wood [10]. The lower EMW absorption in the MG-SB 5% wood is also reportedly due to the cracks and breakage of the coated magnetite surface by EDTA, which reduces the ferrimagnetic phase of the magnetite nanoparticles and makes them more likely to aggregate in the wood pores. This finding is consistent with the results of the VSM and Tesla meter analyses, which showed that the MG-WB 5% wood has higher magnetic properties. The conductivity and electrical polarization of magnetic wood when exposed to a magnetic fluid are also influenced by the chemical components of the wood, which can cause variations in its magnetic properties. Magnetic wood is highly sought after for use in electronic devices such as inductors, transformers, sensors, and electromagnetic interference (EMI) suppressors, among other components, due to the foregoing properties. These properties, together with its initial permeability, flux density, Curie temperature, and low power loss, are crucial factors in determining its suitability for these applications.

4. Conclusion

Magnetic wood was effectively prepared through the impregnation treatment of magnetite nanoparticles that were synthesized using strong base NaOH and weak base NH4OH as precursors. The average particle sizes produced were 103 and 98 nm, respectively. The enhancement of the physical properties of jabon wood by various parameters with increasing nanoparticle concentration was demonstrated through indicators such as WPG, BE, ASE, WU, and wood density. The SEM-EDX analysis revealed magnetite nanoparticles in jabon wood cavities. According to the XRD spectra, the crystallinity of cellulose was also improved, followed by the appearance of new peaks in FTIR that suggest the Fe-O functional group. Excellent magnetic properties were also demonstrated using the three analysis instruments: the Tesla meter, VSM, and VNA. The MG-SB 5% wood absorbed EMWs at a rate of up to 94.71%, while the MG-WB 5% wood absorbed these waves at a rate of 95.55%. It can be inferred that the most effective treatments for converting jabon wood into high-quality magnetic wood are MG-SB 5% and MG-WB 5%. In addition, it is expected that magnetic jabon wood may possess additional functions beyond its capacity as a lightweight construction material, specifically as an EMW-absorbing substance.

References

[1] BI W., LI H., HUI D., GAFF M., LORENZO R., CORBI I., CORBI O., and ASHRAF M. Effects of chemical modification and nanotechnology on wood properties. *Nanotechnology Reviews*, 2021, 10(1): 978-1008. https://doi.org/10.1515/ntrev-2021-0065

[2] GARSKAITE E., STOLL S. L., FORSBERG F., LYCKSAM H., STANKEVICIUTE Z., KAREIVA A., QUINTANA A., JENSEN C. J., LIU K., and SANDBERG D. The Accessibility of the Cell Wall in Scots Pine (Pinus Sylvestris L.) Sapwood to Colloidal Fe3O4 Nanoparticles. *ACS Omega*, 2021, 6(33): 21719–21729. https://doi.org/10.1021/acsomega.1c03204

[3] DONG Y., YAN Y., ZHANG Y., ZHANG S., and LI J. Combined treatment for conversion of fast-growing poplar wood to magnetic wood with high dimensional stability. *Wood Science and Technology*, 2016, 50(3): 503–517. https://doi.org/10.1007/s00226-015-0789-6

[4] WAHYUNINGTYAS I., RAHAYU I. S., MADDU A., and PRIHATINI E. Magnetic properties of wood treated with nano-magnetite and furfuryl alcohol impregnation. *BioResources*, 2022, 17(4): 6496–6510. https://doi.org/10.15376/biores.17.4.6496-6510

[5] LAKSONO G. D., RAHAYU I. S., KARLINASARI L., DARMAWAN W., and PRIHATINI E. Characteristics of magnetic sengon wood impregnated with nano Fe_3O_4 and furfuryl alcohol. *Journal of the Korean Wood Science and Technology*, 2023, 51(1): 1–13. https://doi.org/10.5658/WOOD.2023.51.1.1

[6] FADIA S. L., RAHAYU I., NAWAWI D. S., ISMAIL R., and PRIHATINI E. The Physical and Magnetic Properties of Sengon (Falcataria moluccana Miq.) Impregnated with Synthesized Magnetite Nanoparticles. *Jurnal Sylva Lestari*, 2023, 11(3): 408–426. https://doi.org/10.23960/jsl.v11i3.761

[7] KONG I., AHMAD S. H., ABDULLAH M. H., HUI D., YUSOFF A. N., and PURYANTI D. Magnetic and Microwave Absorbing Properties of Magnetite–Thermoplastic Natural Rubber Nanocomposites. *Journal of Magnetism and Magnetic Materials*, 2010, 322: 3401–3409. https://doi.org/10.1016/j.jmmm.2010.06.036

[8] JAYAPRAKASH J., SRINIVASAN N., and CHANDRASEKARAN P. Surface modifications of CuO nanoparticles using ethylene diamine tetra acetic acid as a capping agent by sol–gel routine. *Spectrochimica Acta Part A: Molecular and Biomolecular Spectroscopy*, 2014, 123: 363–368. https://doi.org/10.1016/J.SAA.2013.12.080

[9] WANG J., LIU J., LI J., and ZHU J. Y. Characterization of Microstructure, Chemical, and Physical Properties of Delignified and Densified Poplar Wood. *Materials*, 2021, 14(19): 5709. https://doi.org/10.3390/ma14195709

[10] PETERNELE W. S., MONGE FUENTES V., FASCINELI M. L., RODRIGUES DA SILVA J., SILVA R. C., LUCCI C. M., and DE AZEVEDO R. B. Experimental Investigation of the Coprecipitation Method: An Approach to Obtain Magnetite and Maghemite Nanoparticles with Improved Properties. *Journal of Nanomaterials*, 2014, 2014(1): 682985. https://doi.org/10.1155/2014/682985

[11] DAOUSH W. M. Co-Precipitation and Magnetic Properties of Magnetite Nanoparticles for Potential Biomedical Applications. *Journal of Nanomedicine Research*, 2017, 5(3): 12–16. https://doi.org/10.15406/jnmr.2017.05.00118

[12] FUMIS D. B., SILVEIRA M. L. D. C., GAGLIERI C., FERREIRA L. T., MARQUES R. F. C., and MAGDALENA A. G. The Effect of EDTA Functionalization on Fe_3O_4 Thermal Behavior. *Materials Research*, 2022, 25: e20220312. https://doi.org/10.1590/1980-5373-MR-2022-0312

[13] KHAN I., SAEED K., and KHAN I. Nanoparticles: Properties, applications and toxicities. *Arabian Journal of Chemistry*, 2019, 12(7): 908-931. https://doi.org/10.1016/j.arabjc.2017.05.011

[14] MARTAWIJAYA A., HADJODARSONO S., and HAJI M. *Atlas Kayu Indonesia Jilid II*. Pusat Penelitian dan Pengembangan Hutan dan Konservasi Alam, Bogor, 2005.

[15] ZHENG D., DONG R., LI Q., and QIU X. Investigation on the binding force between lignin and magnetic Fe_3O_4 nanoparticles with AFM. *Applied Surface Science*, 2021, 538: 148146. https://doi.org/10.1016/j.apsusc.2020.148146

[16] SULISTIO Y., FEBRYANO I. G., YOO J., KIM S., LEE S., HASANUDIN U., and HIDAYAT W. Effects of Torefaction with Counter-Flow Multi Baffle (COMB) Reactor and Electric Furnace on the Properties of Jabon (Anthocephalus Cadamba) Pellets. *Jurnal Sylva Lestari*, 2020, 8(1): 65-76. https://doi.org/10.23960/jsl1865-76

[17] XUE F., & ZHAO G. Optimum preparation technology for Chinese fir wood/Ca-montmorillonite (Ca-MMT) composite board. *Forestry Studies in China*, 2008, 10(3): 199-204. https://doi.org/10.1007/s11632-008-0039-1

[18] RAHAYU I., PRIHATINI E., ISMAIL R., DARMAWAN W., KARLINASARI L., and LAKSONO G. D. Fast-Growing Magnetic Wood Synthesis by an In-Situ Method. *Polymers*, 2022, 14(11): 2137. https://doi.org/10.3390/polym14112137

[19] COATES J. Interpretation of Infrared Spectra, A Practical Approach. In: MEYERS R. A., & MCKELVY M.

L. (eds.) *Encyclopedia of Analytical Chemistry*. 1st ed. Wiley, 2000. https://doi.org/10.1002/9780470027318.a5606
[20] HAZARIKA A., & MAJI T. K. Modification of softwood by monomers and nanofillers. *Defence Science Journal*, 2014, 64(3): 262-272. https://doi.org/10.14429/dsj.64.7325
[21] MAYERHÖFER T., & POPP J. The Electric Field Standing Wave Effect in Infrared Transflection Spectroscopy. *Spectrochimica Acta Part A: Molecular and Biomolecular Spectroscopy*, 2018, 191: 283-289. https://doi.org/10.1016/j.saa.2017.10.033
[22] OSMAN A. I., BLEWITT J., ABU-DAHRIEH J. K., FARRELL C., AL-MUHTASEB A. H., HARRISON J., and ROONEY D. W. Production and characterisation of activated carbon and carbon nanotubes from potato peel waste and their application in heavy metal removal. *Environmental Science and Pollution Research*, 2019, 26(2): 37228–37241. https://doi.org/10.1007/s11356-019-06594-w
[23] DONG Y., YAN Y., ZHANG S., and LI J. Wood/Polymer Nanocomposites Prepared by Impregnation with Furfuryl Alcohol and Nano-SiO2. *BioResources*, 2014, 9(4): 6028–6040. https://doi.org/10.15376/biores.9.4.6028-6040
[24] JAKOB M., MAHENDRAN A. R., GINDL-ALTMUTTER W., BLIEM P., KONNERTH J., MÜLLER U., and VEIGEL S. The strength and stiffness of oriented wood and cellulose-fibre materials: A review. *Progress in Materials Science*, 2022, 125: 100916. https://doi.org/10.1016/j.pmatsci.2021.100916
[25] SOMPECH S., SRION A., and NUNTIYA A. The effect of ultrasonic treatment on the particle size and specific surface area of LaCoO3. *Procedia Engineering*, 2012, 32: 1012-1018. https://doi.org/10.1016/j.proeng.2012.02.047
[26] GAO H. L., WU G. Y., GUAN H. T., and ZHANG G. L. In situ preparation and magnetic properties of Fe3O4/wood composite. *Materials Technology*, 2012, 27(1): 101–103. https://doi.org/10.1179/175355511X13240279339806
[27] NYPELÖ T. Magnetic cellulose: Does extending cellulose versatility with magnetic functionality facilitate its use in devices? *Journal of Materials Chemistry C*, 2022, 10(3): 805–818. https://doi.org/10.1039/d1tc02105b
[28] MOYA R., GAITÁN-ÁLVAREZ J., BERROCAL A., and MERAZZO K. J. In Situ Synthesis of Fe3O4 Nanoparticles and Wood Composite Properties of Three Tropical Species. *Materials*, 2022, 15(9): 3394. https://doi.org/10.3390/ma15093394
[29] PRIHATINI E., WAHYUNINGTYAS I., RAHAYU I. S., and ISMAIL R. Pengaruh Larutan Furfuril Alkohol dan Nanopartikel SiO2 pada Beberapa Metode Impregnasi Kayu Jabon. *Indonesian Journal of Laboratory*, 2023, 6(3): 7–13. https://doi.org/10.22146/ijl.v0i3.84108
[30] JOHN S. P., & MATHEW J. Superparamagnetism of Mg0.5Zn0.5Fe2O4 nanoparticles: Dependence of pH in the sol-gel auto-combustion method. *AIP Conference Proceedings*, 2019, 2162: 020066. https://doi.org/10.1063/1.5130276
[31] PRIHATINI E., WAHYUNINGTYAS I., RAHAYU I., and ISMAIL R. Modification of Fast-Growing Wood into Magnetic Wood with Impregnation Method Using Fe3O4 Nanoparticles. *Jurnal Sylva Lestari*, 2022, 10(2): 211-222. https://doi.org/10.23960/jsl.v11i2.651
[32] FADIA S. L., RAHAYU I., NAWAWI D. S., ISMAIL R., and PRIHATINI E. Magnetic characteristics of sengon wood-impregnated magnetite nanoparticles synthesized by the co-precipitation method. *AIMS Materials Science*, 2024, 11(1): 1-27. https://doi.org/10.3934/matersci.2024001
[33] SITORUS Z., HAKIM L., SIHOMBING F. A., and SIHOMBING A. T. Influence of Micro Structure Based Magnetic Material BaNixAl6-xFe6O19 as Material Absorber Wave Magnetic Structure. *Journal of Physics: Conference Series*, 2018, 1116: 032036. https://doi.org/10.1088/1742-6596/1116/3/032036
[34] JOHAN A., SETIABUDIDAYA D., ARSYAD F. S., MASHADI, SARWANTO Y., WINATAPURA D. S., TARYANA Y., YUNASFI, and ADI W. A. Magnetic and Microwave Absorbing Properties in Semi-Hard CoxFe(3-x)O4 Synthesized by Sol-Gel Method. *Jurnal Teknologi*, 2023, 85(4): 199–204. https://doi.org/10.11113/jurnalteknologi.v85.17741
[35] SILVIA L., ASLAMA B., NOVIALENT E., and ZAINURI M. Synthesis of Magnetite Fe3O4 from Laterite Iron Rock as Microwave Absorber Material. *Journal of Physics: Conference Series*, 2021, 1951(1): 012024. https://doi.org/10.1088/1742-6596/1951/1/012024

参考文:

[1] BI W.、LI H.、HUI D.、GAFF M.、LORENZO R.、CORBI I.、CORBI O. 和 ASHRAF M. 化学改性和纳米技术对木材特性的影响。纳米技术评论，2021 年，10(1)：978-1008。https://doi.org/10.1515/ntrev-2021-0065
[2] GARSKAITE E.、STOLL S. L.、FORSBERG F.、LYCKSAM H.、STANKEVICIUTE Z.、KAREIVA A.、QUINTANA A.、JENSEN C. J.、LIU K. 和 SANDBERG D. 苏格兰松(樟子松)边材细胞壁对胶体氧化铁纳米粒子的可及性。美国癌症协会欧米茄，2021，6(33)：21719–21729。https://doi.org/10.1021/acsomega.1c03204
[3] DONG Y.、YAN Y.、ZHANG Y.、ZHANG S. 和 LI J. 联合处理将速生杨木转化为高尺寸稳定性磁性木材。木材科学与技术，2016，50(3)：503–517。https://doi.org/10.1007/s00226-015-0789-6
[4] WAHYUNINGTYAS I.、RAHAYU I. S.、MADDU A. 和 PRIHATINI E. 经纳米磁铁矿和糠醇浸渍处理木材的磁性。生物资源，2022，17(4)：6496–6510。https://doi.org/10.15376/biores.17.4.6496-6510
[5] LAKSONO G. D.、RAHAYU I. S.、KARLINASARI L.、DARMAWAN W. 和 PRIHATINI E. 用纳米氧化铁和糠醇浸渍的磁性先根木材的特性。韩国木材科学与技术杂志，2023，51(1)：1–13。https://doi.org/10.5658/WOOD.2023.51.1.1
[6] FADIA S. L.、RAHAYU I.、NAWAWI D. S.、ISMAIL R. 和 PRIHATINI E. 浸渍合成磁铁矿纳米粒子的仙贡（南洋杉.）的物理和磁性。西尔瓦·莱斯塔里杂志，2023，11(3)：408–426。https://doi.org/10.23960/jsl.v11i3.761

[7] KONG I.、AHMAD S. H.、ABDULLAH M. H.、HUI D.、YUSOFF A. N. 和 PURYANTI D. 磁铁矿-热塑性天然橡胶纳米复合材料的磁性和微波吸收性能。《磁学与磁性材料杂志》，2010 年，第 322 期：第 3401-3409 页。https://doi.org/10.1016/j.jmmm.2010.06.036

[8] JAYAPRAKASH J. 、SRINIVASAN N. 和 CHANDRASEKARAN P. 使用乙二胺四乙酸作为封端剂通过溶胶-凝胶法对氧化铜纳米粒子进行表面改性。《光谱化学学报》一个部分：分子和生物分子光谱学，2014 年，第 123 期：第 363-368 页。https://doi.org/10.1016/J.SAA.2013.12.080

[9] WANG J.、LIU J.、LI J. 和 ZHU J. Y. 脱木素和致密化杨木的微观结构、化学和物理特性表征。材料，2021，14(19)：5709。https://doi.org/10.3390/ma14195709

[10] PETERNELE W. S.、MONGE FUENTES V.、FASCINELI M. L.、RODRIGUES DA SILVA J.、SILVA R. C.、LUCCI C. M. 和 DE AZEVEDO R. B. 共沉淀法实验研究：一种获得性能改进的磁铁矿和磁赤铁矿纳米粒子的方法。《纳米材料杂志》，2014 年，2014(1)：682985。https://doi.org/10.1155/2014/682985

[11] DAOUSH W. M. 磁铁矿纳米粒子的共沉淀和磁性及其在生物医学应用方面的潜在价值。《纳米医学研究杂志》，2017 年，5(3)：12–16。https://doi.org/10.15406/jnmr.2017.05.00118

[12] FUMIS D. B.、SILVEIRA M. L. D. C.、GAGLIERI C.、FERREIRA L. T.、MARQUES R. F. C. 和 MAGDALENA A. G. 乙二胺四乙酸功能化对氧化铁热行为的影响。材料研究，2022，25：e20220312。https://doi.org/10.1590/1980-5373-MR-2022-0312

[13] KHAN I.、SAEED K. 和 KHAN I. 纳米粒子：特性、应用和毒性。阿拉伯化学杂志，2019，12(7)：908-931。https://doi.org/10.1016/j.arabjc.2017.05.011

[14] MARTAWIJAYA A.、HADJODARSONO S. 和 HAJI M. 印度尼西亚地方地图集 II。土壤和地下水管理中心，茂物，2005 年。

[15] ZHENG D.、DONG R.、LI Q. 和 QIU X. 使用 AFM 研究木质素与磁性氧化铁纳米粒子之间的结合力。应用表面科学，2021 年，538：148146。https://doi.org/10.1016/j.apsusc.2020.148146

[16] SULISTIO Y.、FEBRYANO I. G.、YOO J.、KIM S.、LEE S.、HASANUDIN U. 和 HIDAYAT W. 使用逆流多挡板(梳子)反应器和电炉进行焙烧对豇豆属（卡丹巴花）颗粒性能的影响。西尔瓦·莱斯塔里杂志，2020，8(1)：65-76。https://doi.org/10.23960/jsl1865-76

[17] 薛峰，赵刚。杉木/钙蒙脱石（钙蒙脱土）复合板最佳制备工艺。中国林业研究，2008，10(3)：199-204。https://doi.org/10.1007/s11632-008-0039-1

[18] RAHAYU I.、PRIHATINI E.、ISMAIL R.、DARMAWAN W.、KARLINASARI L.、LAKSONO G. D. 采用原位法合成快速生长磁性木材。聚合物，2022，14(11)：2137。https://doi.org/10.3390/polym14112137

[19] COATES J. 红外光谱解释，一种实用方法。在：MEYERS R. A. 和 MCKELVY M. L.（编辑）《分析化学百科全书》。第一版。威利，2000 年。https://doi.org/10.1002/9780470027318.a5606

[20] HAZARIKA A. 和 MAJI T. K. 单体和纳米填料对软木的改性。国防科学杂志，2014，64(3)：262-272。https://doi.org/10.14429/dsj.64.7325

[21] MAYERHÖFER T. 和 POPP J. 红外透射光谱中的电场驻波效应。光谱化学学报一个：分子和生物分子光谱，2018，191：283-289。https://doi.org/10.1016/j.saa.2017.10.033

[22] OSMAN A. I.、BLEWITT J.、ABU-DAHRIEH J. K.、FARRELL C.、AL-MUHTASEB A. H.、HARRISON J. 和 ROONEY D. W. 利用马铃薯皮废料生产活性炭和碳纳米管及其在重金属去除中的应用。环境科学与污染研究，2019，26(2)：37228–37241。https://doi.org/10.1007/s11356-019-06594-w

[23] DONG Y.、YAN Y.、ZHANG S. 和 LI J. 通过用糠醇和纳米二氧化硅浸渍制备木材/聚合物纳米复合材料。生物资源，2014 年，9(4)：6028–6040。https://doi.org/10.15376/biores.9.4.6028-6040

[24] JAKOB M.、MAHENDRAN A. R.、GINDL-ALTMUTTER W.、BLIEM P.、KONNERTH J.、MÜLLER U. 和 VEIGEL S. 定向木材和纤维素纤维材料的强度和刚度：综述。材料科学进展，2022，125：100916。https://doi.org/10.1016/j.pmatsci.2021.100916

[25] SOMPECH S.、SRION A. 和 NUNTIYA A. 超声波处理对钴酸镧粒径和比表面积的影响。普罗西迪亚工程公司，2012，32：1012-1018。https://doi.org/10.1016/j.proeng.2012.02.047

[26] GAO H. L.、WU G. Y.、GUAN H. T. 和 ZHANG G. L. 氧化铁/木材复合材料的原位制备及磁性能。材料技术，2012，27(1)：101-103。https://doi.org/10.1179/175355511X13240279339806

[27] NYPELÖ T. 磁性纤维素：通过磁性功能扩展纤维素的多功能性是否有助于其在设备中的使用？《材料化学杂志碳》，2022 年，10(3)：805–818。https://doi.org/10.1039/d1tc02105b

[28] MOYA R.、GAITÁN-ÁLVAREZ J.、BERROCAL A. 和 MERAZZO K. J. 三种热带物种的氧化铁纳米粒子的原位合成和木材复合材料性能。材料，2022, 15(9): 3394。https://doi.org/10.3390/ma15093394

[29] PRIHATINI E.、WAHYUNINGTYAS I.、RAHAYU I. S. 和 ISMAIL R. 糠醇溶液和二氧化硅纳米颗粒对几种贾本木材浸渍方法的影响。印度尼西亚实验室杂志，2023，6(3)：7–13。https://doi.org/10.22146/ijl.v0i3.84108

[30] JOHN S. P., & MATHEW J. 镁锌铁氧体纳米颗粒的超顺磁性：溶胶-凝胶自燃烧法中 pH 值的依赖性。急性内窥镜检查会议论文集，2019 年，2162：020066。https://doi.org/10.1063/1.5130276

[31] PRIHATINI E.、WAHYUNINGTYAS I.、RAHAYU I. 和 ISMAIL R. 使用氧化铁纳米粒子通过浸渍法将速生木材改性为磁性木材。西尔瓦·莱斯塔里杂志，2022 年，10(2)：211-222。https://doi.org/10.23960/jsl.v11i2.651

[32] FADIA S. L.、RAHAYU I.、NAWAWI D. S.、ISMAIL R. 和 PRIHATINI E. 通过共沉淀法合成的先根木材浸渍磁铁矿纳米粒子的磁性特征。目标材料科学，2024，11(1)：1-27。https://doi.org/10.3934/matersci.2024001

[33] SITORUS Z.、HAKIM L.、SIHOMBING F. A. 和 SIHOMBING A. T. 微结构基磁性材料 BaNixAl6-xFe6O19 作为材料吸收波磁结构的影响。物理学杂志：会议系列，2018 年，1116：032036。https://doi.org/10.1088/1742-6596/1116/3/032036

[34] JOHAN A.、SETIABUDIDAYA D.、ARSYAD F. S.、MASHADI、SARWANTO Y.、WINATAPURA D. S.、TARYANA Y.、YUNASFI 和 ADI W. A. 溶胶-凝胶法合成的半硬钴铁氧体的磁性和微波吸收特性。工艺学杂志，2023 年，85(4)：199–204。https://doi.org/10.11113/jurnalteknologi.v85.17741

[35] SILVIA L.、ASLAMA B.、NOVIALENT E. 和 ZAINURI M. 从红土铁岩合成磁铁矿氧化铁作为微波吸收材料。《物理学杂志：会议系列》，2021 年，1951(1)：012024。https://doi.org/10.1088/1742-6596/1951/1/012024